Supporting Information to

Fast and one-step fabrication of vertically-ordered mesoporous silica-nanochannel film on graphene for direct and sensitive detection of doxorubicin in human whole blood

Fei Yan,[a,‡] Jie Chen,[b,‡] Qifan Jin,[a] Huaxu Zhou,[a] Ajab Khan Sailjoi,[a] Jiyang Liu,[a,*] Weizhong Tang[b,*]

[a] Department of Chemistry, Zhejiang Sci-Tech University, 928 Second Avenue, Xiasha Higher Education Zone, Hangzhou, 310058, PR China

[b] Guangxi Medical University, 22 Shuangyong Road, Nanning 530021, PR China

‡ These two authors contributed equally

* Corresponding author. E-mail: tangweizhong@gxmu.edu.cn; liujy@zstu.edu.cn

Table of Contents

S1. Molecular structure of DOX

Scheme S1. Molecular structure of DOX.

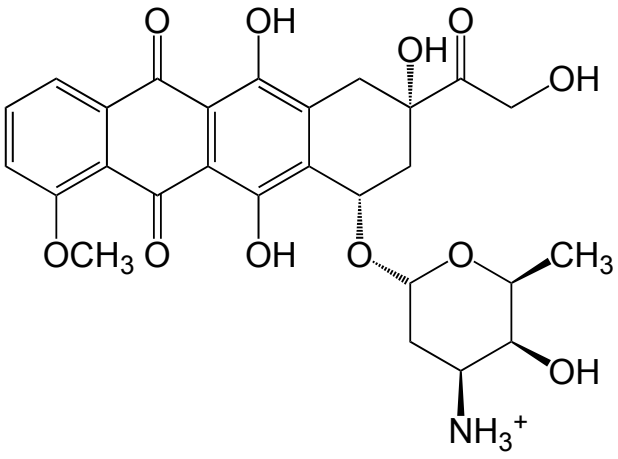

S2. Preparation and Characterizations of VMSF/ErGO/GCE

S2.1 *i-t* response of the preparation of VMSF/GCE and VMSF/ErGO/GCE by EASA

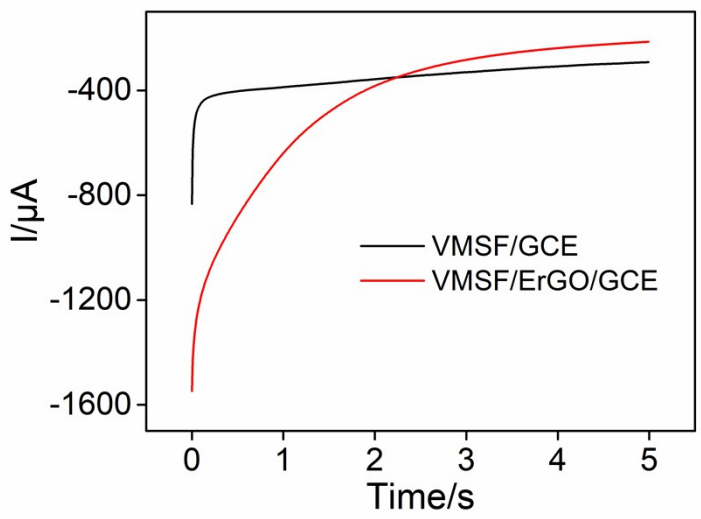

Fig. S1 The *i-t* curves of the preparation of VMSF/GCE and VMSF/ErGO/GCE by EASA method. The applied potential was –2.2 V.

S2.2 Raman of GO and ErGO

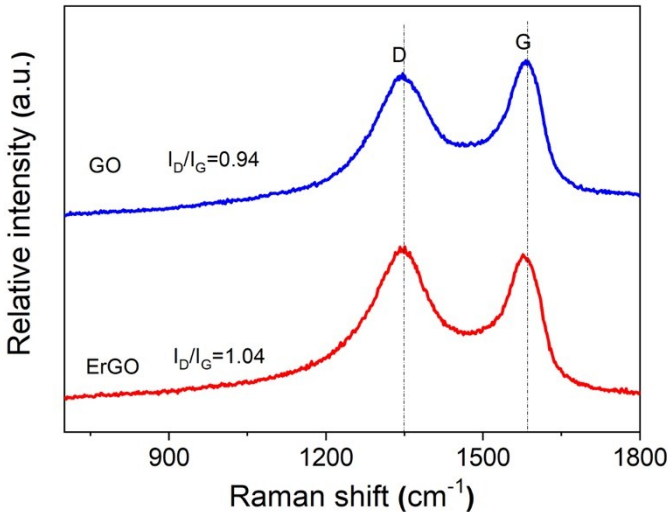

Fig. S2 Raman spectra of GO and ErGO.

S2.3 Stability of VMSF/ErGO/GCE

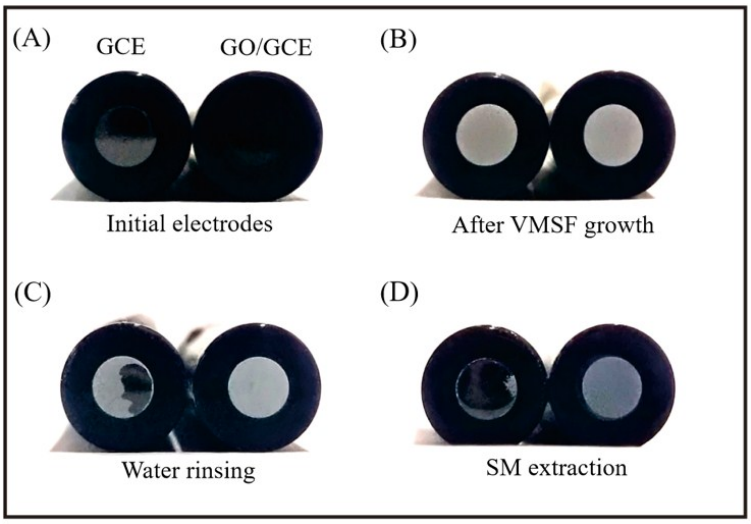

Fig. S3 Photographs of bare GCE and GO/GCE (a), SM@VMSF/GCE and SM@VMSF/ErGO/GCE before (b) and after rinsing by water (c) or HCl-ethanol solution (d). VMSF/GCE and VMSF/ErGO/GCE were obtained after the removal of SM from nanochannels by using HCl-ethanol solution.

S2.3 EIS characterization of VMSF/ErGO/GCE

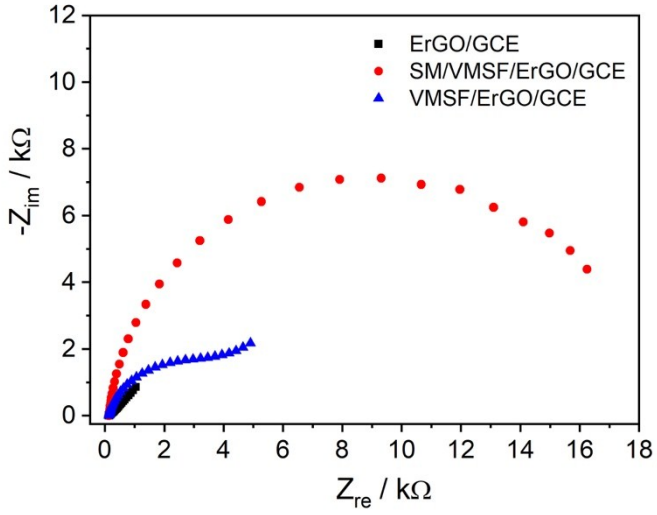

Fig. S4 EIS plots of ErGO/GCE, SM/VMSF/ErGO/GCE and VMSF/ErGO/GCE. EIS experiments were conducted in 0.05 M M KHP solution containing 2.5 mM $K_3Fe(CN)_6$ and 2.5 mM $K_4Fe(CN)_6$.

S3. CVs of DOX at the VMSF/APTES/GCE and APTES/GCE

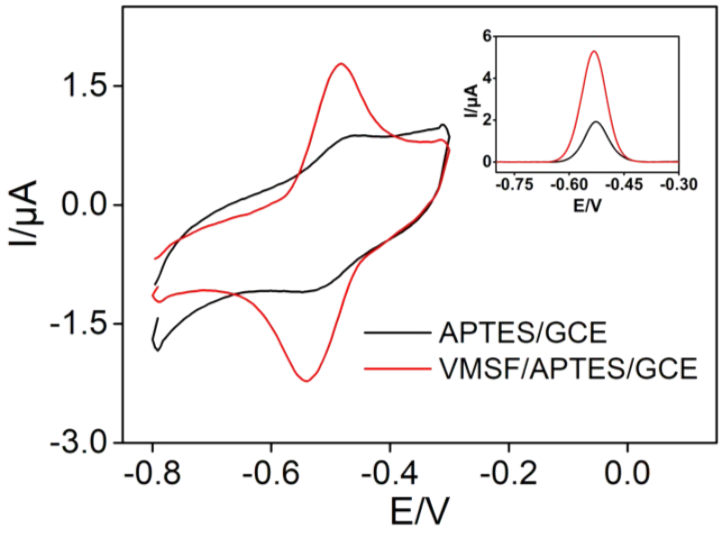

Fig. S5 CV curves obtained from APTES/GCE and VMSF/APTES/GCE in 0.1 M PBS (pH = 6.0) containing 10 μM DOX. The inset was the corresponding DPV curves.

S4. The effect of scan rate on the CV responses

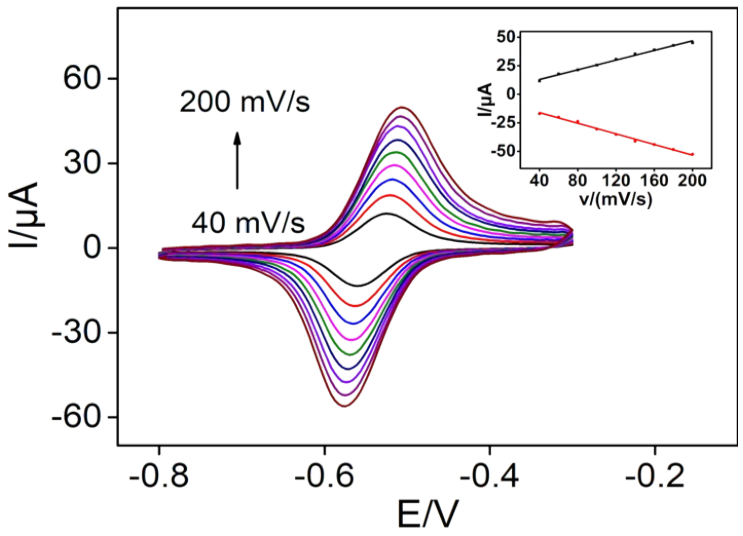

Fig. S6 CV curves obtained from VMSF/ErGO/GCE in PBS (0.1 M, pH 6.0) containing 10 μM DOX at different scan rates. The inset was the dependence of anodic and cathodic peak potential on scan rate.

S5. CVs of APAP, Trp and UA at the VMSF/ErGO/GCE

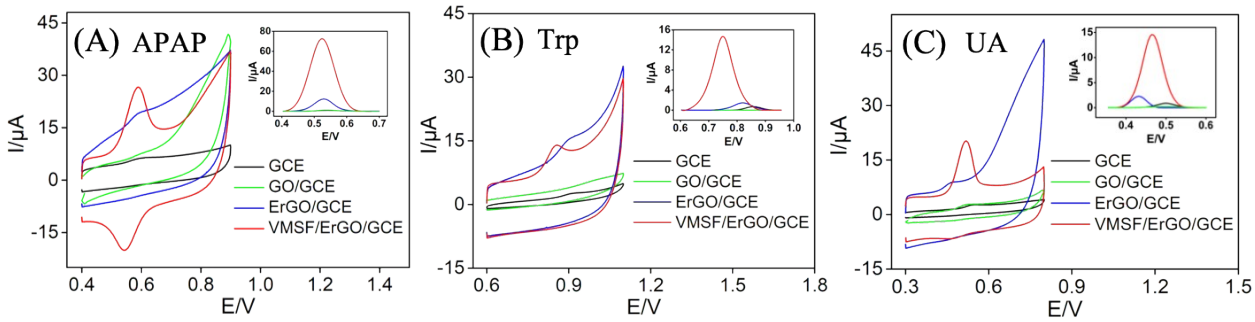

Fig. S7 CV curves of 20 μM APAP (A), Trp (B) and UA (C) at the GCE, GO/GCE, ErGO/GCE, and VMSF/ErGO/GCE in 0.1 M PBS solution (pH = 4.0). The scan rate was 100 mV/s. The insets were corresponding DPV curves.

S6. Optimized conditions for electrochemical detection

S6.1. Applied potential and applied time

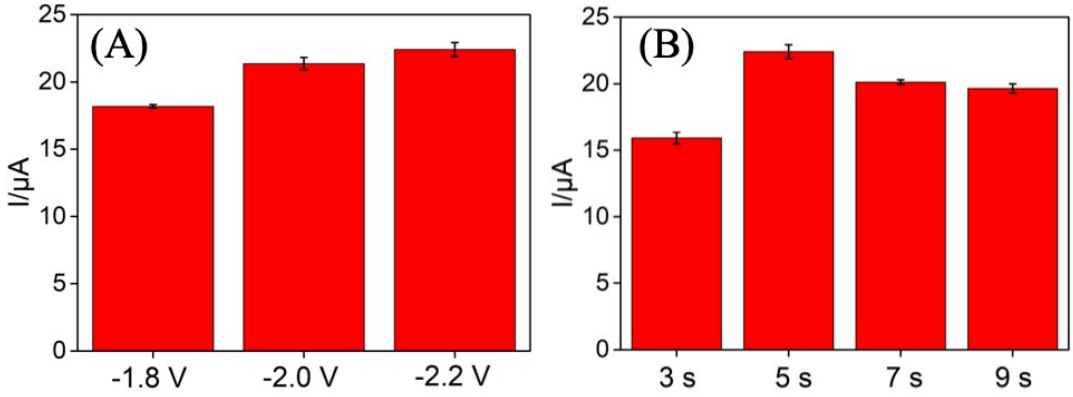

Fig. S8 Effect of applied potential (A) and applied time (B) on the current response of 3 μM DOX in PBS (0.1 M, pH 6.0). In (A) applied time 5 s; in (B) applied potential −2.2 V.

S6.2 pH of supporting electrolyte

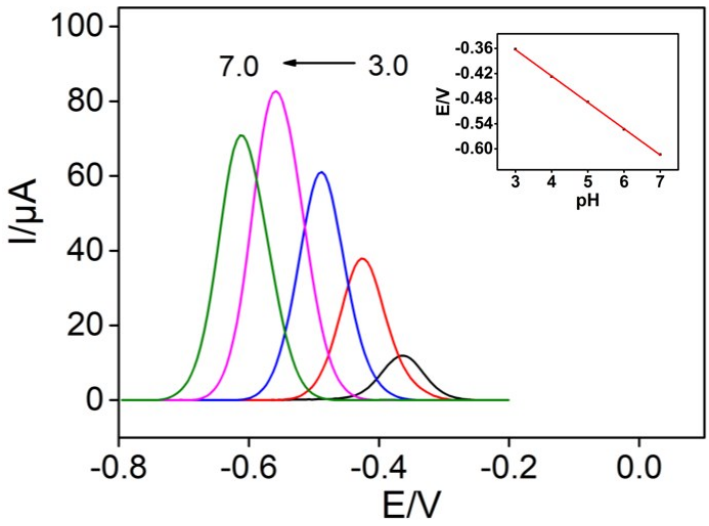

Fig. S9 DPV curves for VMSF/ErGO/GCE in 0.1 M PBS containing 10 μM DOX at various pH values. The inset shows the linear dependence of anodic peak potential (*E*) on pH value.

S6.3 Preconcentration time

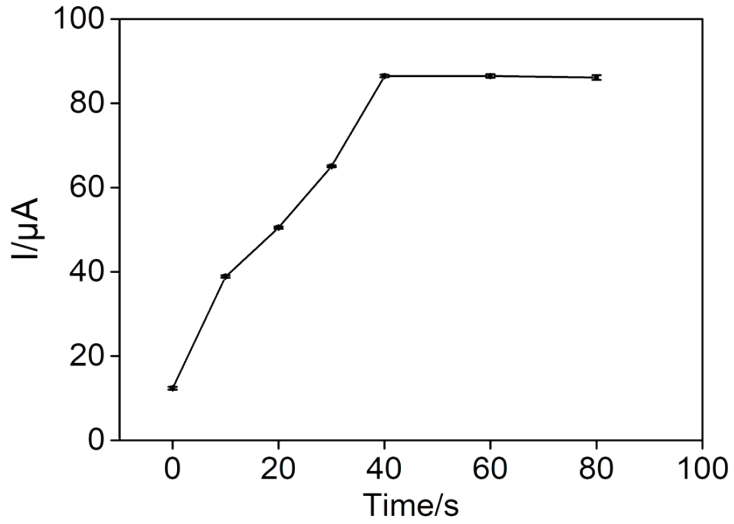

Fig. S10 Influence of the stirring time on the current response of 10 μM DOX in 0.1 M PBS (pH = 6.0). The error bars represent the standard deviations of three measurements.

S7. Comparison of various electrodes for electrochemical detection of DOX

Table S1. Comparison of the analytical performance of the VMSF/ErGO/GCE with other electrodes for the electrochemical detection of DOX in PBS solution

Electrode	Sensitivity (μA/μM)	Range (μM)	LOD (nM)	*R*
VMSF/ErGO/GCE	7.815	0.001−20	0.77	0.9993
ErGO/GCE	2.422	0.5−20	33.5	0.9995
GCE	0.6168	1−15	532	0.9991
VMSF/APTES/GCE	0.4753	1−20	623	0.9968